QUANTITATIVE ANALYSIS OF CONCRETE ON THE BASIS OF FUZZY SET AND COMPUTERISED TOMOGRAPHY NUMBER

by

Jian-Yin FANG[a*], Na LI[a], Fei QU[a], Zhan-Shuang DOU[b], and Shu-Tian LI[a]

[a] State Key Laboratory of Eco-Hydraulics in Northwest Arid Region, Xi'an University of Technology, Xi'an, China
[b] Ning Xia Ccommunications Cconstruction CO., LTD, China

Original scientific paper
https://doi.org/10.2298/TSCI2006907F

In this study, the portable power loading device and medical Marconi M8000 spiral CT scanner are used to conduct the uniaxial compression CT scanning test of the concrete. The concrete porosity, hardened cement rate, and aggregate rate are defined, and the variation law of the concrete is analyzed in the uniaxial compression CT test. The proposed method is considered to utilize the value of each CT number, to realize the quantitative partition of the various components of concrete, and to quantitatively evaluate the damage evolution law of the concrete and strain localization during stress. It is shown that damage at the middle section increased from inside to the outside in the uniaxial compression CT test of the concrete.

Key words: *hydraulic material, quantitative subarea, concrete CT test, fuzzy set, porosity*

Introduction

The X-ray computed tomography (CT) scanning technology has the advantages of non-destructive detection of the 3-D microscopic mechanism of the materials [1, 2]. It is widely used in the mesoscopic research on rock and concrete [3-5]. The changes in the internal structure of concrete during cement hydration by means of X-ray CT scanning were studied in [6]. The fracture mode of a concrete surface based on X-ray CT equipment was analyzed in [7]. The development of internal cracks in mortar samples by X-ray CT scanning equipmentstudied in [8, 9]. The isolation resistance, strength response and accelerated corrosion of self-compacting lightweight concrete by using CT technology and fractal theory is evaluated in [10]. A number of literatures on the quantitative analysis of the consequence of the material failure are available in the current CT test of rock and concrete based on observation and mathematical statistics methods [11-13]. However, the literature on the quantitative analysis of the process of material failure is few.

Therefore, studying the damage mechanism of rock by image analysis is difficult. A partition method based on fuzzy set and CT number is proposed. Furthermore, the strength characteristics and damage evolution of concrete during uniaxial compression CT test are quantitatively studied.

* Corresponding author, e-mail: fjylxr@163.com

Uniaxial compression CT test

Test conditions

The portable power loading equipment developed by Xi'an University of Technology and the Marconi M8000 spiral CT scanner are used in the experiment, the image size of which is 512 × 512 CT units, and the maximum imaging speed of four layers can be scanned within 0.5 s. The loading equipment and scanning position are shown in fig. 1.

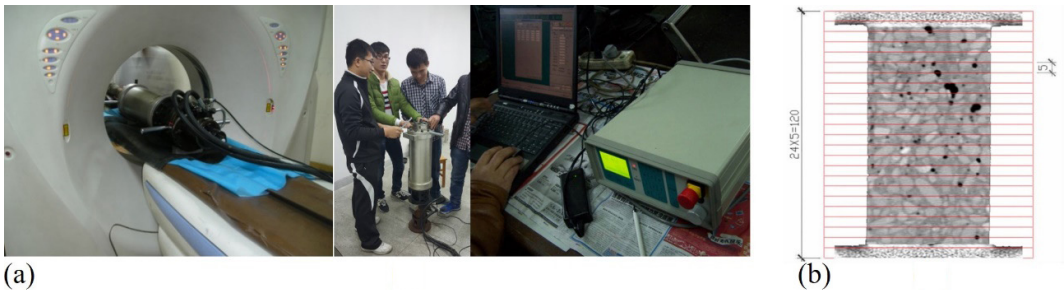

Figure 1. Portable dynamic loading equipment and CT scan localization; (a) portable dynamic loading equipment and (b) the CT scan localization of the sample

The cylindrical specimen of the test, with a size of ∅60 mm × 120 mm, is made of the first grade C15 concrete. The gravel aggregate particle size is 5-20 mm. The mixture ratio of concrete is as follows: the water-cement ratio is 0.62 and the sand rate is 45%. The water consumption in one cubic meter of concrete is 170 kg. The cement consumption in one cubic meter of concrete is 274 kg. The fine aggregate consumption in one cubic meter of concrete is 870 kg. The coarse aggregate consumption in one cubic meter of concrete is 1062 kg. The test is carried out under standard conditions for 28 days.

Test procedure

In the test, the portable loading device is placed in the center of the CT scanner in the hospital. The scanning layers of the sample are 24 in the horizontal direction, and each layer is evenly arranged according to the sample. Initial scanning is performed. The initial scanning diagram of the sample serves as the basis for the comparison of image changes. Then, the stress uniaxial compressive strength of concrete specimens should be pre-estimated to determine the number of scanning load steps. The load control is initially adopted with 60 kN and loading rate of 0.2 kN/s. Then, loading is stopped with unchanged displacement. After the completion of all steps, the second scanning can be performed. Subsequently, displacement loading mode is adopted at the loading rate of 0.002 mm/s. When the specimen is broken, the experiment is over. Through the experiment, the peak load of the sample can be obtained at 101.98 kN. The loading is stopped at each scan and repeated in the sequence of loading, scanning, continuing loading and scanning until the concrete is destroyed, and the loading is stopped. During the entire test, a total of 10 scans are performed.

Test results

The uniaxial compression CT scanning test indicates that hundreds of CT scanning images of different interfaces and stress stages of concrete can be obtained. The CT scans are shown in fig. 2. In the figure, the higher density indicates a larger CT number, and the white on the scans represents the aggregate. The smaller density indicates the smaller CT number,

and the black on the scans represents the hole crack. The grey, between the white and the black, is the product of hydration hardening of cement. In this article, it is called *hardened cement stone*.

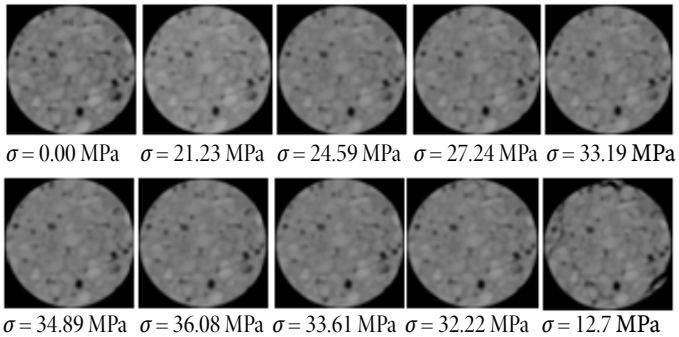

Figure 2. Scan of section one at each loading stage

Division theory

Damage-fracture space

The CT number of each resolution point in the CT scan of concrete is clear in its physical definition. The CT number of each resolution point represents the density of the point at the current stress level. The change of the CT number at the point throughout the loading process implies the change of the degree of the integrity (integrity, damage and fracture). However, the change of CT number in the CT scan is randomly distributed and has no continuity. In order to determine the law of change, it is necessary to introduce the concept of *set*.

Integrity

The entire concrete samples are called the entire domain. Set $\Omega = \{(x, y, z) \mid (x, y, z)\}$ is the arbitrary point on the object space of the research. From the point of view of fuzzy mathematics, every point in the entire domain is complete, but the integrity is not the same. On this basis, the integrity of concrete is defined as follows:

$$p(x, y, z) = \frac{H(x, y, z) + 1000}{\max H(x, y, z) + 1000} \tag{1}$$

where $H(x, y, z)$ is the CT number at a point (x, y, z) in the study domain.

The CT number at a point is expressed:

$$H(x, y, z) = \frac{\mu_t - \mu_w}{\mu_w} \cdot 1000 \tag{2}$$

where μ_t and μ_w represent the X-ray linear attenuation coefficients of the corresponding minerals and water in the scanned images.

The level complete domain and intercepted section

The concrete is a multiphase inhomogeneous material with pore and initial defects. The concept of integrity blurs the integrity, damage and fracture of the research domain. It cannot be used to clearly describe the specific changes of the aggregate, hardened cement, pores and initial defects. Thus, introducing a complete domain and intercepted section is necessary.

Let $0 \le \lambda \le 1$. The λ-level complete domain of the specimen, denoted as denoted as P_λ, is $\{(x, y, z) \mid \lambda \le P(x, y, z) \le 1, (x, y, z) \in \Omega\}$. The intercepted section in complete domain, denoted as $P_{\lambda_1 - \lambda_2}$, is $\{(x, y, z) \mid \lambda_1 \le P(x, y, z) \le \lambda_2, (x, y, z) \in \Omega$, and $0 \le \lambda_1 \le \lambda_2 \le 1\}$. The complete domain and intercepted section are two subsets of Ω.

Figure 3 shows the complete domain and intercepted section for a cross-section of the concrete specimen. It is shown that as long as the value of λ is appropriately selected, $P_{0-\lambda_1}$

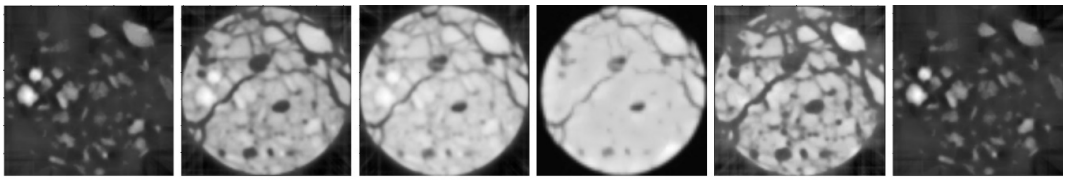

(a) $P = 0.85$ (b) $P = 0.75$ (c) $P = 0.65$ (a') $P = 0\text{-}0.65$ (b') $P = 0.65\text{-}0.85$ (c') $P = 0.85\text{-}1$

Figure 3. Complete domain and intercepted sections

represents the set of all CT points, and it density is less than a certain threshold, which is the crack area. Therefore, the λ-level damage domain of the specimen can be regarded as the damage zone of the classical damage mechanics or the crack of the fracture mechanics. The concrete scan can be divided into the hole-crack area, hardened cement area, and aggregate area by intercepted section.

Quantitative partition and threshold determination

The concrete is a multiphase composite material that comprises aggregates, including coarse and fine aggregates, initial hole-cracks and hardened cement stone. The CT number of each resolution cell in the specimen varies with increasing load. We divide the concrete into aggregate area, hardened cement zone and the hole-crack zone by mean of the complete domain and intercepted section.

The specific cases are as follows:

- When $0 \le P(x, y, z) < \lambda_1$, the material is believed to contain pores or fractured. It is called the hole-crack area, denoted as $P_{0-\lambda_1}$.
- When $\lambda_1 \le P(x, y, z) < \lambda_2$, the material integrity is considered general, and the material is in the hardened cement zone, denoted as $P_{\lambda_1-\lambda_2}$.
- When $\lambda_2 \le P(x, y, z) \le 1$, the material integrity is high in the aggregate area (coarse and fine aggregates) , denoted as P_{λ_2-1}.

Here, λ_1 is the threshold of the crack zone and the hardened cement zone, and λ_2 is the threshold of the hardened cement and aggregate areas.

Quantitative description of concrete damage evolution process

The regional change rate based on the entire domain

The statistical analysis of the cross-sections of the concrete under the uniaxial stress level shows that the relationship among $n_{0-\lambda_1}$, $n_{\lambda_1-\lambda_2}$, and n_{λ_2-1} with the number of scanning sections is shown in figs. 4 and 5, respectively.

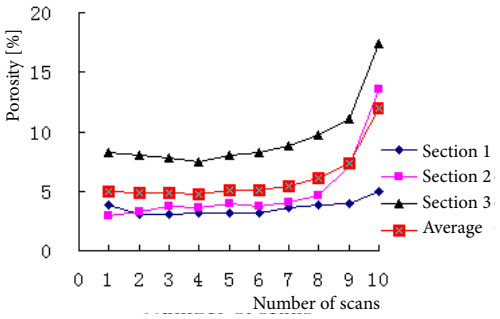

Figure 4. Change of $n_{0-\lambda_1}$ with scanning frequency

Figure 4 shows that the process of each section of the sample differs with increasing loading scanning. The parameter $n_{0-\lambda_1}$ of Sections 1 and 3 has undergone a small reduction, a slow increase and a jump-like process, whereas the parameter $n_{0-\lambda_1}$ of Section 2 only experiences a slow increase to a leap-type increase process. The minimum value of the parameter $n_{0-\lambda_1}$ of Section 1 appears at the third scan, and the minimum value of the parameter $n_{0-\lambda_1}$ of Section 3 appears at the fourth scan with values of 3.07% and 7.45%, respectively.

Moreover, the parameter $n_{0-\lambda_1}$ decreases by 0.77% and 0.79%, respectively. The process of decreasing of the parameter $n_{0-\lambda_1}$ reflects the process of the sample being compacted. This process weakens the injury. The essence of this phenomenon is that the initial defects (damage), such as holes and microcracks in the scanned section of the concrete specimen, appear to close under the action of pressure, and the specimen is compacted. The reduction in the parameter $n_{0-\lambda_1}$ represents the amount of pressure in this section of the sample. In the process from the minimum value of $n_{0-\lambda_1}$ to the fifth scan (load is 33.19 MPa), the parameter $n_{0-\lambda_1}$ slightly increases, and the average $n_{0-\lambda_1}$ increment is only 0.03% for the three sections. At this stage, the microscopic damage of the specimens is insignificant, and the concrete material is in the elastic deformation stage.

The change of aggregate rate with loading can also reflects the damage process of materials. The variation rule of aggregate rate according to the CT scan test is shown in fig. 5. It shows that the variation law of the parameter n_{λ_2-1} on each section is consistent, and the variation rule of n_{λ_2-1} is opposite to the parameter $n_{0-\lambda_1}$ with loading. With the loading scan, a small increase of the parameter n_{λ_2-1} initially appears and then slowly decreases. At the last step of loading scan, the parameter n_{λ_2-1} shows a large jump in terms of decrease. The change process of n_{λ_2-1} with loading scan can also reflect that the sample undergoes the process of compaction, expansion and failure under compression. Prior to the third scan (24.59 MPa), the initial crack of the sample closes with increasing load. The parameter $P_{\lambda_1-\lambda_2}$ is transformed into P_{λ_2-1} (32.22 MPa). The CT number of a point is affected by the CT number of nearby points, and an increase in the parameter n_{λ_2-1} is observed. The process from the third loading scan to the ninth loading scan (32.22 MPa) is the load expansion stage of the sample. During this process, the aggregate is damaged due to failure under load. At the 10th loading scan, the parameter n_{λ_2-1}shows a jump decrease. Thus, when concrete is destroyed under compression, a large number of aggregate is suddenly destroyed, and the parameter P_{λ_2-1} s is sharply reduced. Furthermore, n_{λ_2-1} shows a jump decrease.

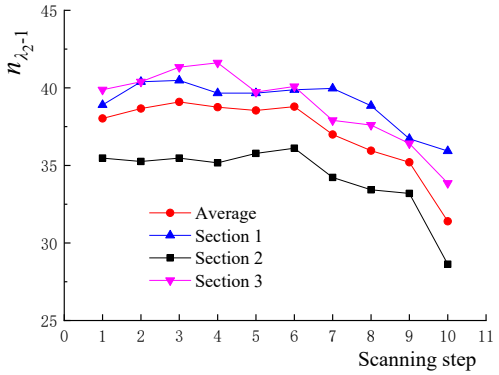

Figure 5. Change of n_{λ_2-1} with the scanning step

For the nonhomogeneous concrete material with the initial defects, the strain process has certain strain localization, and the damage of each part of the sample section differs. To identify the localization of the strain and the specific law of the damage evolution, we consider the cross-section of concrete specimen division. Therefore, the CT scan images of concrete are evenly divided into six concentric ring regions (represented by H1-H6). The division of the regions is based on CT point co-ordinates with the aid of the program of the FORTRAN software.

It is indicated that the variation law of the parameter $n_{0-\lambda_1}$ can better reflect the damage evolution law of the crack in the process of concrete stress. Therefore, the parameter $n_{0-\lambda_1}$ increment is used as the parameter to study the local damage. The analysis of Sections 2 and 3 is carried out, and the test results are shown in fig. 6.

Comparing the graphs in figs. 6(a) and 6(b), the test process is divided into four stages for analysis. The first stage comprises the first to the fourth scans (0-27.24 MPa). The second stage comprises the fourth to the sixth scan (27.24-34.89 MPa), the third stage is the sixth to the seventh scan (34.89-36.08 MPa), and the fourth stage is the seventh to the 10th scan (36.08-12.7 MPa).

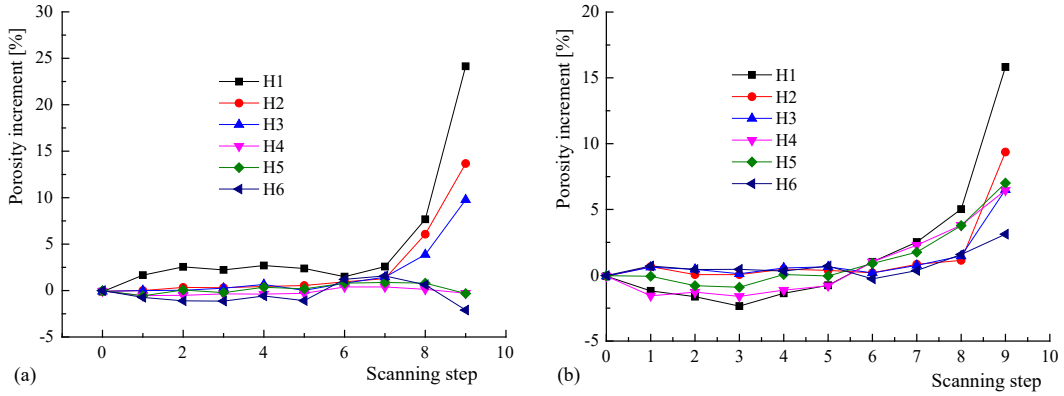

Figure 6. Increment change of $n_{0-\lambda_1}$ with scanning frequency; (a) Section 2 and (b) Section 3

Figure 6(a) shows that for Section 2, the parameter $\Delta n_{0-\lambda_1}$ of the H4 and H6 statistical area is –0.27% and –1.02%, respectively. The parameter $\Delta n_{0-\lambda_1}$ of H1 statistical area is 2.34%, whereas in the other three statistical areas, the change of the parameter $\Delta n_{0-\lambda_1}$ is small mainly because the initial crack in the middle part of the sample in this stage is closed under compression. Thus, the number of the parameter $P_{0-\lambda_1}$ is reduced, where the parameter $n_{0-\lambda_1}$ is reducing. Therefore, the first stage can be considered the small amount of compaction stage. In the second stage, with increasing loading displacement, the parameter $\Delta n_{0-\lambda_1}$ increases slowly in the fluctuation. The load reaches the peak intensity of 36.08 MPa, the parameter $\Delta n_{0-\lambda_1}$ of each statistical area is larger than 0 and more concentrated.

Figure 6(b) shows that the regularity of Section 3 in the earlier stage is exactly the same as that of Section 2. In Section 3, the regularity of the sample is different from that in Section 2 in the stage of instability and failure. This finding is mainly manifested in the distribution of the parameter $P_{0-\lambda_1}$ and the value size of the parameter $\Delta n_{0-\lambda_1}$.

Conclusion

In the task, the partitioning method based on the fuzzy set and CT number was proposed for first time. This method can be used to divide the concrete CT image into a hole-crack area, hardened cement rate and aggregate area. Then porosity of the concrete, the hardening rate of cement stone and the aggregate rate were considered in detail. The problem of the quantitative analysis of the concrete CT test results was solved. It accurately reflected the crack increment and aggregate damage amount. It is shown that the cross-section of the concrete sample under the uniaxial compression goes through the compaction-expansion-failure process, and that the damage is increased from inward to outward in the mid-section.

Acknowledgment

The research is funded by the Natural Science Foundation of China (No. 51679199), Natural Science Foundation of Shaanxi Provincial Department of Education of China (No. 18JK0547), Science and technology innovation project of Xi'an university of Technology (No.2016CX026) and Xi'an university of Technology School Doctor Gold (No.107-451116012).

References

[1] Daisuke, F., *et al.*, Investigation of Self-Sealing in Highstrength and Ultra-Low-Permeability Concrete in Water Using Micro-Focus Xray CT, *Cement and Concrete Research*, *45* (2020), 39, pp. 20240-20249

[2] Xue, Y., *et al.*, Productivity Analysis of Fractured Wells in Reservoir of Hydrogen and Carbon based on Dual-Porosity Medium Model, *International Journal of Hydrogen Energy*, *45* (2020), 39, pp. 20240-20249
[3] Rougelot, T., *et al*., About Microcracking Due to Leaching in Cementitious Composites, X-Ray Microtomography Description and Numerical Approach, *Cem Concr Res*, *40* (2010), 2, pp. 271-283
[4] Xue, Y., *et al.*, Analysis of Deformation, Permeability and Energy Evolution Characteristics of Coal Mass around Borehole after Excavation, *Natural Resources Research*, *29* (2020), 5, pp. 3159-3177
[5] Promentilla, M., *et al*., Quantification of Tortuosity in Hardened Cement Pastes Using Synchrotron-Based X-Ray Computed Microtomography, *Cem. Concr. Res.*, *39* (2009), 6, pp. 548-557
[6] Chotard, T. J., *et al*., Application of X-ray Computed Tomography to Characterise the Early Hydration of Calcium Aluminate Cement, *Cement and Concrete Composites*, *25* (2003), 1, pp. 145-152
[7] John, S. L., *et al*., Measuring Three-Dimensional Damage in Concrete Under Compression, *Materials Journal*, *98* (2001), 6, pp. 465-475
[8] Landis, E. N., *et al*., Microstructure and Fracture in Three Dimensions, *Engineering Fracture Mechanics*, *70* (2003), 7-8, pp. 911-925
[9] Elaqra, H., *et al*., Damage Evolution Analysis in Mortar, during Compressive Loading Using Acoustic Emission and X-Ray Tomography: Effects of the Sand/Cement Ratio, *Cement and Concrete Research*, *37* (2007), 5, pp. 703-713
[10] Savas, E., X-ray Computed Tomography and Fractal Analysis for the Evaluation of Segregation Resistance, Strength Response and Accelerated Corrosion, *Construction and Building Materials*, *61* (2014), June, pp. 10-17
[11] Liu, J., *et al.*, Numerical Evaluation on Multiphase Flow and Heat Transfer during Thermal Stimulation Enhanced Shale Gas Recovery, *Applied Thermal Engineering*, *178* (2020), Sept., pp. 115554
[12] Xue, Y., *et al.*, Numerical Investigation of Effects of Heat Injection Enhanced Methane Recovery on Groundwater Loss, *Science of the Total Environment*, (2021), pp. 1-10
[13] Gallucci, E., *et al*., 3D Experimental Investigation of the Microstructure of Cement Pastes Using Synchrotron X-Ray Microtomography, *Cem. Concr. Res, 37* (2007), 3, pp. 360-368

Paper submitted: March 6, 2020
Paper revised: May 28, 2020
Paper accepted: August 9, 2020